

A Study on the Effect of Neighboring Protons in Proton-Coupled Spin-Lattice Relaxation of Methylene Carbon-13 in *n*-Undecane

Chul Kim and Jo Woong Lee*

School of Chemistry, College of Natural Sciences, Seoul National University, Seoul 151-742, Korea

Received January 14, 2002

Proton coupled carbon-13 relaxation experiment was performed to investigate the effect of *vicinal* protons on spin-lattice relaxation of methylene carbon-13 in *n*-undecane. A BIRD type pulse sequence was employed as a way to check the validity of describing the $^{13}\text{CH}_2$ moiety as an isolated AX_2 spin system. The results show that the presence of *vicinal* protons exerts substantial influence on the relaxation of methylene carbon-13, indicating that it is not a very good approximation to treat a methylene moiety as an isolated AX_2 spin system.

Keywords : Proton-coupled relaxation, *n*-Undecane, Deuteration, BIRD-pulse.

Introduction

The knowledge of dynamics of methylene moieties is of crucial importance for better understanding of the segmental motions occurring in a long hydrocarbon chain and the study of proton-coupled relaxation of carbon-13 in CH_2 groups can serve usefully for this purpose.¹⁻¹² In particular, for an *n*-alkane chain molecule, dipole-dipole spectral densities obtained from the proton-coupled carbon-13 relaxation experiments provide us a valuable insight into the segmental motions occurring in the straight carbon backbone.

Grant and coworkers as well as Fuson *et al.* utilized the proton-coupled carbon-13 relaxation as a means of investigating the segmental motions in *n*-nonane labeled at the central carbon.¹¹ In order to analyze the observed curves for several relaxation modes they treated the methylene moiety at the central carbon as an isolated AX_2 spin system and regarded the protons two bonds away from the carbon of interest, which will, for brevity, be henceforth referred to as *vicinal* protons, merely as a source of random field. Surprisingly, when theoretical calculations based on the Redfield equation were performed for the AX_2 spin system, this oversimplified view, however, was found to lead to a good fit with experimental data, thus yielding a set of values for various spectral densities. When the *vicinal* protons were deuterated to minimize the effect originating from them, the theoretical relaxation curves could also be fitted well with the observed ones, but yielding a somewhat different set of values for the dipolar spectral densities.¹¹ This means that the assumption that the interaction with *vicinal* protons may be treated only as a random field term is not very satisfactory and, whenever possible, the deuteration of interfering protons is recommended. Since deuteration of a proton (or protons) at a given carbon site is very laborious and time-consuming, use of the deuterated sample is not always practical and/or feasible.

In the present work we explore a new BIRD-type pulse experiment, besides that employed by Grant *et al.*,¹² to

tackle this problem. A BIRD pulse is applied to *n*-undecane to invert only those protons directly bonded to the methylene carbon of interest (henceforth referred to as *geminal* protons).¹³ Relaxation from the initial spin state created in this manner was also observed in addition to those obtained by the conventional Grant method. Simultaneous fitting of these two different types of relaxation curves will obviously give us more leverage to determine the set of values of spectral densities than relying only on the Grant type measurements. Not surprisingly, theoretical calculation based on the AX_2 model with the effect of *vicinal* protons being treated as a random field term failed to produce a good simultaneous fit with these two different types of relaxation data. To analyze the situation we assumed that the system may be described as an AX_2M system, where the *geminal* protons, X_i , are assumed to be weakly coupled to a *vicinal* proton, M , and kept only the dominating terms representing the effect due to the latter protons in the corresponding relaxation matrix. Of course, there are four *vicinal* protons around a given methylene carbon but we assume their effect may be described by considering only one of them when they are motionally equivalent. This situation will ideally suit for the central carbon site in a hydrocarbon chain. However, if the carbon site of interest is very close to the center of the chain, the same approximation is expected to be equally well valid as we demonstrate in this paper. An AX_2M model was found to be able to describe both of the two different kinds of experimental data satisfactorily, thus producing a reliable set of parametric values for spectral densities. Hopefully, when generalized, we may employ this method as a routine substitute of expensive and painstaking course of deuteration in the study of segmental motions in the chain molecules.

Theory

Bloch-Redfield theory. The fundamental equation of motion for a nuclear spin system can be derived from the time-dependent Schrödinger equation. The second-order perturbation theory leads to the so-called Redfield equation

*Corresponding author. E-mail: jwlee@mmlab2.snu.ac.kr

for the spin density operator:^{14,15}

$$\frac{d\sigma_{kk}^{(r)}}{dt} = \sum_{\lambda\lambda'} e^{i(k-k'-\lambda+\lambda')t} R_{kk'\lambda\lambda'} [\sigma_{\lambda\lambda'}^{(r)}(t) - \sigma_{\lambda\lambda'}^{(r)}(\infty)], \quad (1)$$

where the elements of the relaxation matrix \mathbf{R} depends on the dipole-dipole and random field spectral densities. When only the longitudinal spin components are relevant, one may use a simpler form of Eq. (1) which can be rewritten in the following form of Solomon equation:¹⁶

$$\frac{dN_i}{dt} = \sum_j W_{ij} [N_j(t) - N_j(\infty)], \quad (2)$$

where $N_i(t)$ and $N_i(\infty)$ are, respectively, the population of the i th spin energy level at time t and at equilibrium and W_{ij} is the rate for transition $j \rightarrow i$. For convenience Eq. (2) may also be written in terms of the symmetrized normal modes as have been shown by Grant *et al.*, which involves the normalized irreducible tensor operators. Grant *et al.* have defined a normal magnetization mode as the trace over product of deviation density operator with a corresponding irreducible spherical tensor operator.¹⁷⁻²⁰ In this formalism each normal magnetization mode can be expressed as a linear combination of the diagonal density-matrix elements and among them as many modes as possible are experimentally measured and compared with theoretically derived expressions.

For our study of a $^{13}\text{CH}_2$ moiety in n -undecane we will briefly outline the application of this formalism to AX_2 and AX_2M spin system. The energy levels and eigenstates for an AX_2 system are as shown in Figure 1. For this spin system symmetric and antisymmetric normal magnetization modes are expressed as follows:

$$\begin{aligned} v_1 &= \frac{1}{2}(N_1 - N_2 + N_3 + N_4 - N_5 - N_6 - N_7 - N_8) \\ &= (L_1 + L_2 - L_3)/2k_A \equiv v_{+++} \end{aligned}$$

$$v_2 = \frac{1}{\sqrt{2}}(N_1 + N_2 - N_7 - N_8) - (L_4 + L_5)/\sqrt{2}k_A \equiv v_{-}$$

$$\begin{aligned} v_3 &= \frac{1}{2}(N_1 - N_2 - N_3 - N_4 - N_5 - N_6 + N_7 - N_8) \\ &= (L_1 - L_2 - L_3)/2k_A \equiv v_{-} \end{aligned}$$

$$v_4 = \frac{1}{\sqrt{2}}(N_3 - N_4 - N_5 - N_6) \quad (3)$$

$$\begin{aligned} v_5 &= \frac{1}{\sqrt{2}}(N_1 - N_2 - N_7 + N_8) - (L_1 - L_5)/\sqrt{2}k_A \\ &- (L_4 - L_3)/\sqrt{2}k_A \equiv v_{10-} \end{aligned}$$

$$v_6 = \frac{1}{2}(N_1 + N_2 - N_3 - N_4 - N_5 - N_6 + N_7 + N_8)$$

$$v_7 = \frac{1}{\sqrt{2}}(N_3 - N_4 - N_5 + N_6)$$

$$v_8 = N_1 + N_2 + N_3 - N_4 - N_5 + N_6 + N_7 + N_8 = N_{total} \equiv v_T$$

and the equation of motion for these magnetization modes is

$$\frac{dv_i}{dt} = - \sum_j \Gamma_{ij} [v_j(t) - v_j(\infty)], \quad (4)$$

where the matrix Γ is blockdiagonalized into ${}^o\Gamma$ and ${}^s\Gamma$ and their matrix elements are given as below:

$$\begin{aligned} {}^o\Gamma_{11} &= 20/3 J_{CH} + 2j_C & {}^o\Gamma_{12} &= 5\sqrt{2}/3 J_{CH} & {}^o\Gamma_{13} &= 2J_{HH} \\ {}^o\Gamma_{14} &= 7\sqrt{2}/3 J_{HH} \\ {}^o\Gamma_{22} &= 10/3 J_{CH} - 5J_{HH} + 2j_H & {}^o\Gamma_{23} &= 2\sqrt{2} J_{CH} \\ {}^o\Gamma_{24} &= 5/3 J_{HH} - 2J_{CH} \\ {}^o\Gamma_{33} &= 4J_{CH} + 2J_{HH} - 2j_C + 4j_H \\ {}^o\Gamma_{34} &= -\sqrt{2} J_{CH} - \sqrt{2} J_{HH} - 2\sqrt{2} j_{HH} \\ {}^o\Gamma_{44} &= 14/3 J_{CH} - 4/3 J_{HH} + J_{HH} + 2j_C + 4j_H - 2j_{HH} \\ {}^s\Gamma_{11} &= 16/3 J_{CH} - 2J_{HH} + 5J_{HH} + 2j_C + 2j_H \\ {}^s\Gamma_{12} &= 5\sqrt{2}/3 J_{CH} + 2\sqrt{2} J_{CH} \\ {}^s\Gamma_{13} &= 5/3 J_{HH} - 2J_{CH} \end{aligned}$$

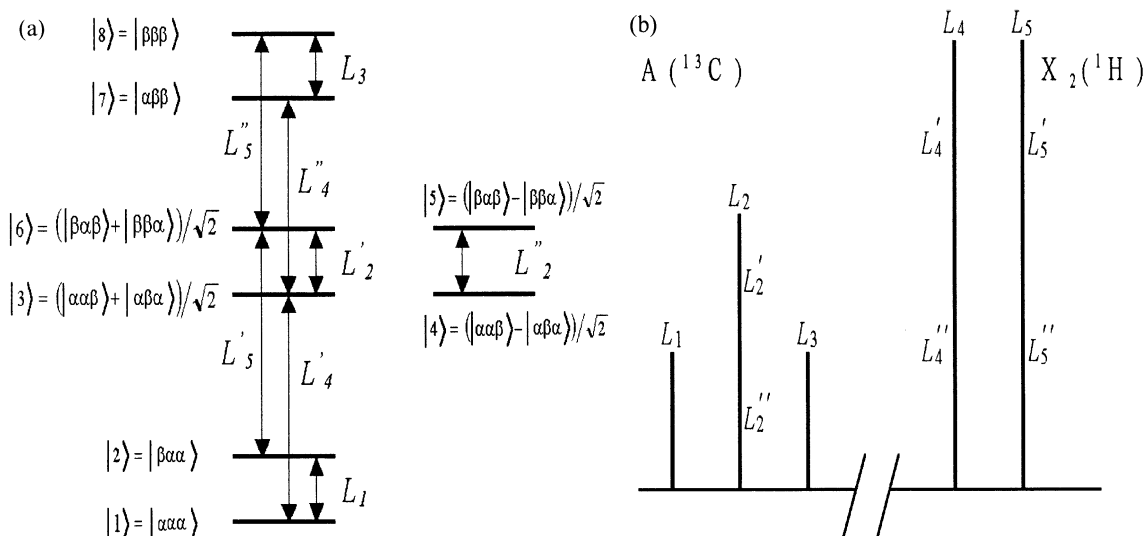


Figure 1. (a) Energy Level Diagram and Eigenstates - spin labels are in the order of C, H, H' spins; L_i 's are the allowed (single quantum) transitions that lead to spectral lines shown in (b); (b) A Schematic Spectrum - triplet for $A(^{13}\text{C})$ and doublet for $X_2(^1\text{H})$ in isotropic media.

$$\begin{aligned}
 {}^1T_{22} &= 20/3J_{CH} + 2J_{HH} + 4j_{H1} \\
 {}^1T_{23} &= 10\sqrt{2}/3J_{HCH} + \sqrt{2}J_{HH} + 2\sqrt{2}j_{H1}, \text{ and} \\
 {}^1T_{33} &= 20/3J_{CH} - 10/3J_{HCH} + J_{HH} + 4j_{H1} - 2j_{H3}
 \end{aligned}
 \tag{5}$$

The matrices 1T and 2T are both symmetric, that is, ${}^1T_{ij} = {}^1T_{ji}$ and ${}^2T_{ij} = {}^2T_{ji}$. In isotropic media only four of the modes given in Eq. (3) are directly measurable. They are ${}^1v_{11}$, the total *A* magnetization; ${}^1v_{1x}$, the total *X* magnetization; ${}^1v_{1-1}$, the difference in intensity between the sum of outer two lines and the inner single line of the *A* triplet, and ${}^1v_{10}$, the difference in intensity between the outer two lines of the *A* triplet.

For methylene moieties in *n*-undecane the chemical shift differences between *geminal* and *vicinal* protons are comparable in magnitude with the scalar spin coupling between them and, therefore, at a first glance we might be tempted to describe these protons as comprising a strongly coupled spin system. However, we can show that the presence of ^{13}C allows us to treat the moiety interacting with a vicinal proton as a weakly coupled AX_2M spin system due to large coupling constant between *A* and *X* spins where *A* stands for ^{13}C and *X* and *M*, respectively, for *geminal* and *vicinal* proton. This means that only the secular term $J_{XM}I_X \cdot I_M$, instead of the full interaction $J_{XM}I_X \cdot I_M$, needs to be considered when dealing with the scalar coupling between the two protons. The neglected nonsecular terms can be shown to generate a small amount of coherences of the type $I_{A-}I_X I_M$ and $I_{A+}I_X I_M$ (involving the zero quantum of the protons *X* and *M*) when a BIRD pulse is applied (See Appendix II). However, this type of coherences was found to quickly decay away (probably due to rapid spin diffusion process of protons) before applying a observing carbon 90° pulse providing no interference with our measurement. In reality, there are four vicinal protons surrounding a given methylene carbon-13 atom in *n*-undecane. But their influences on this carbon-13 atom may be considered approximately additive and can be described

in terms of that of a single proton *M*.

The carbon-13 signal for a $^{13}CH_2$ moiety in *n*-undecane basically consists of three lines with the intensity ratio of 1 : 2 : 1 which are separated from each other by the coupling constant J_{CH} (≈ 125 Hz). In the presence of vicinal protons each of these lines is split further, but the coupling between the carbon-13 and a *vicinal* proton is so small that the splitting due to this coupling was hardly resolvable in our case. Therefore, we had to observe the integrated intensities of these unresolved lines in our experiment, which means that we can treat the dynamics of our methylene moiety in terms of various relaxation modes of an AX_2 system that undergo cross relaxation with the *M* spin. The energy levels and eigenstates for an AX_2M system are as shown in Figure 2.

In dealing with the effect of the *vicinal* protons, we define symmetric and antisymmetric normal magnetization modes for an AX_2M system as follows:

$$\begin{aligned}
 {}^1v_1 &= \frac{1}{2}(N_1 - N_2 - N_3 + N_4 - N_5 - N_6 + N_7 - N_8 + N_9 \\
 &\quad - N_{10} + N_{11} + N_{12} - N_{13} - N_{14} + N_{15} - N_{16}) \equiv {}^1v_{11} \\
 {}^1v_2 &= \frac{1}{\sqrt{2}}(N_1 + N_2 - N_7 - N_8 + N_9 + N_{10} - N_{15} - N_{16}) \equiv {}^1v_{1x} \\
 {}^1v_3 &= \frac{1}{2}(N_1 - N_2 - N_3 - N_4 + N_5 + N_6 + N_7 - N_8 + N_9 \\
 &\quad - N_{10} - N_{11} - N_{12} + N_{13} + N_{14} + N_{15} - N_{16}) \equiv {}^1v_{1-1} \\
 {}^1v_4 &= \frac{1}{\sqrt{2}}(N_3 - N_4 - N_5 - N_6 + N_{11} - N_{12} - N_{13} - N_{14}) \\
 {}^1v_5 &= \frac{1}{\sqrt{2}}(N_1 - N_2 - N_7 + N_8 + N_9 - N_{10} - N_{15} + N_{16}) \equiv {}^1v_{10} \\
 {}^1v_6 &= \frac{1}{2}(N_1 - N_2 - N_3 - N_4 - N_5 - N_6 + N_7 + N_8 + N_9 \\
 &\quad - N_{10} - N_{11} - N_{12} - N_{13} - N_{14} + N_{15} + N_{16})
 \end{aligned}$$

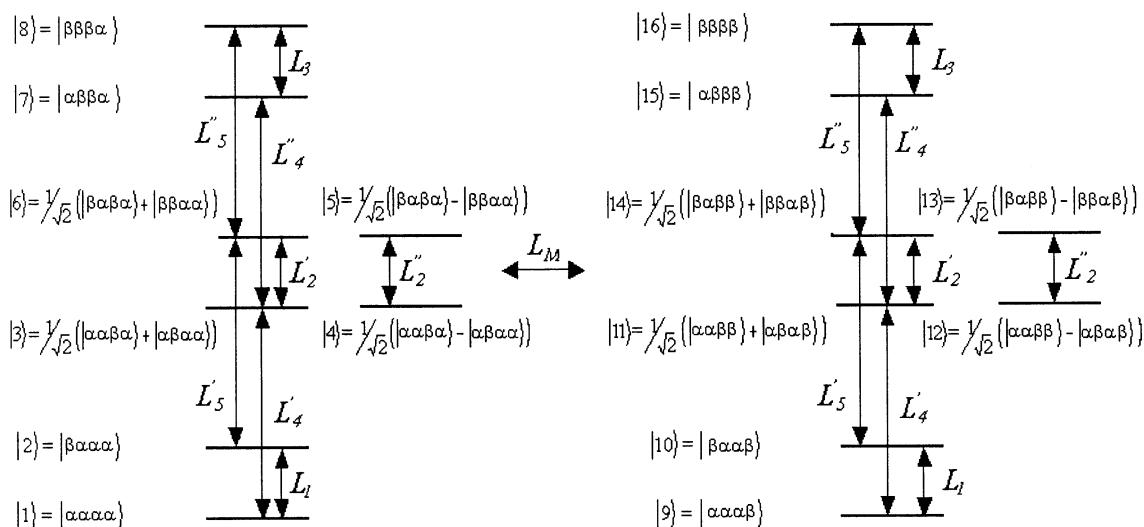


Figure 2. Energy Level Diagram and Eigenstates - spin labels are in the order of C, H, H', M spins; L_i 's and L_M are the allowed (single quantum) transitions of AX_2 spin and *M* spin respectively.

$$\begin{aligned}
 v_7 &= \frac{1}{\sqrt{2}}(N_3 - N_4 - N_5 + N_6 + N_{11} - N_{12} - N_{13} + N_{14}) \\
 v_8 &= N_1 + N_2 + N_3 - N_4 + N_5 + N_6 - N_7 + N_8 + N_9 - N_{10} \\
 &\quad + N_{11} + N_{12} - N_{13} + N_{14} - N_{15} + N_{16} \equiv v_f \\
 v_9 &= \frac{1}{2}(N_1 - N_2 + N_3 + N_4 - N_5 - N_6 + N_7 - N_8 - N_9 - N_{10} \\
 &\quad - N_{11} - N_{12} + N_{13} + N_{14} - N_{15} + N_{16}) \\
 v_{10} &= \frac{1}{\sqrt{2}}(N_1 + N_2 - N_7 - N_8 - N_9 - N_{10} - N_{15} + N_{16}) \\
 v_{11} &= \frac{1}{2}(N_1 - N_2 - N_3 - N_4 + N_5 + N_6 - N_7 - N_8 - N_9 + N_{10} \\
 &\quad + N_{11} + N_{12} - N_{13} - N_{14} - N_{15} + N_{16}) \\
 v_{12} &= \frac{1}{\sqrt{2}}(N_3 - N_4 + N_5 - N_6 - N_{11} - N_{12} - N_{13} + N_{14}) \\
 v_{13} &= \frac{1}{\sqrt{2}}(N_1 - N_2 - N_7 + N_8 - N_9 + N_{10} + N_{15} - N_{16}) \\
 v_{14} &= \frac{1}{2}(N_1 + N_2 - N_3 - N_4 - N_5 - N_6 + N_7 + N_8 - N_9 - N_{10} \\
 &\quad + N_{11} + N_{12} + N_{13} + N_{14} - N_{15} - N_{16}) \\
 v_{15} &= \frac{1}{\sqrt{2}}(N_3 - N_4 - N_5 + N_6 - N_{11} + N_{12} + N_{13} - N_{14}) \\
 v_{16} &= N_1 + N_2 + N_3 + N_4 + N_5 + N_6 - N_7 + N_8 - N_9 - N_{10} \\
 &\quad - N_{11} - N_{12} - N_{13} - N_{14} - N_{15} - N_{16} \equiv v_{Mf} \quad (6)
 \end{aligned}$$

Each of these magnetization modes will relax according to Eq. (4) for which the elements of relaxation matrix Γ are given in Appendix 1. Among these, the modes of our interest are v_1 , the total A magnetization, v_2 , the total X magnetization, v_3 , the difference in integral between the sum of outer two lines and the inner single line of the broad A triplet, v_5 , the difference in integral between the outer two lines of the broad unresolved A triplet, and v_{Mf} , the total M magnetization. The modes v_9 to v_{15} are all the M -related transition modes.

Among the M -related modes by far the most dominant is v_{Mf} mode, because this term remains much larger than the others during the relaxation. So, to a good approximation we may expect the effect of the presence of *vicinal* protons to be accounted for by considering only the cross relaxation between the AX_2 modes and v_{Mf} mode. Evaluation of the relaxation matrix for the weakly coupled AX_2M brought the following facts to our attention. First, for the AX_2M spin system diagonal and cross terms relating the modes (v_1 to v_7) with each other are the same as those for the AX_2 spin system providing the dipolar terms involving M spin are viewed as random field terms. Second, only v_1 and v_3 mode among v_1 to v_7 are influenced by the relaxation of v_{Mf} mode. Third, all the cross relaxation elements between modes related to the transitions for the AX_2 spin system and those for M spin involve cross spectral densities between AX_2 spins and M spin. These elements are expected to be

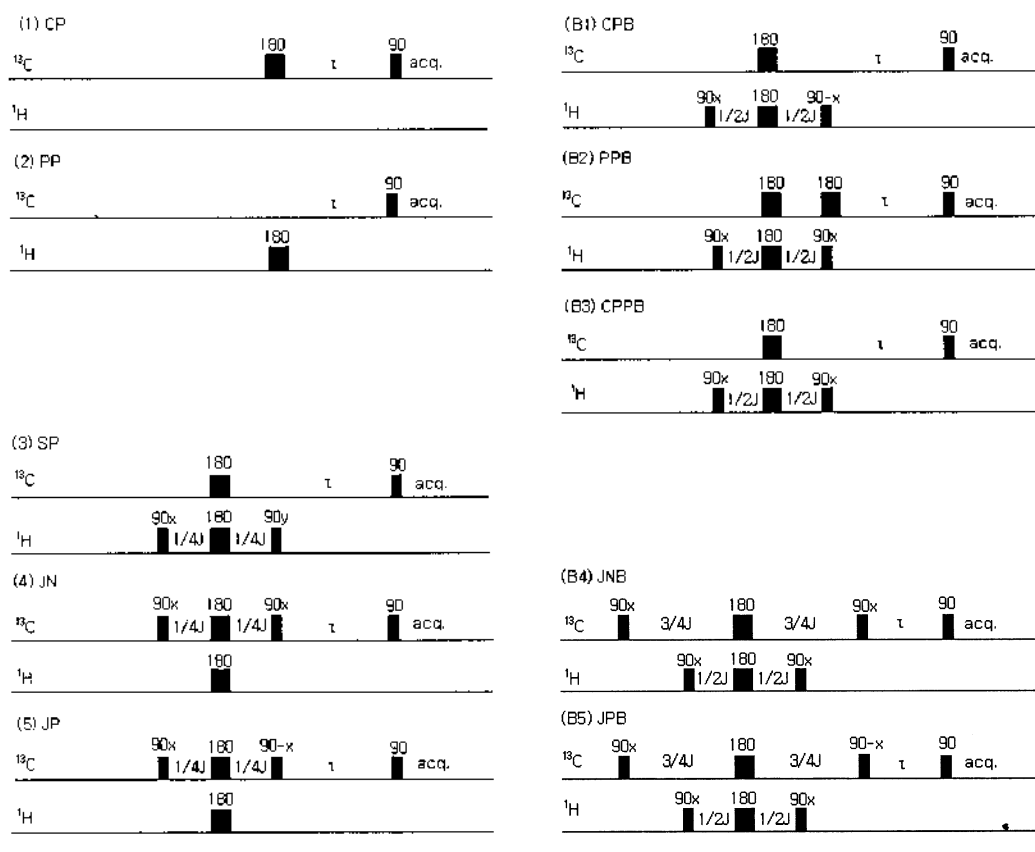


Figure 3. Pulse Sequences Used for Initial Excitation of Observable Magnetization Modes.

small in magnitude considering that the presence of *vicinal* protons provides merely a small perturbation. Since the Grant-type pulse sequences and the BIRD-type pulse sequences both generate almost the same initial states of the *M*-related transition modes, ${}^a\nu_9$ to ${}^a\nu_{15}$, we can safely ignore the cross relaxation terms involving the *M*-related transition modes except ${}^a\nu_M$. Based on this simplified treatment we could successfully fit the derived relaxation curves for various normal modes with the observed ones including those obtained by applying the BIRD-type pulses.

Experimentals and Calculations

Sample. The [5- ^{13}C] *n*-undecane was synthesized in our laboratory. This was dissolved in CDCl_3 and sealed in 5 mm NMR tubes after repeating five freeze-pump-thaw cycles to remove dissolved oxygen. The NMR experiments were performed on an Varian VXR 200S spectrometer operating at a ^{13}C frequency of 50.3 MHz. The temperature was maintained at 298 K throughout the measurements.

Pulses. The Grant pulse sequences invert both *geminal* and *vicinal* protons using a hard 180° proton pulse while in the BIRD-type pulse sequences only the *geminal* protons in $^{13}\text{CH}_2$ moiety are inverted leaving the *vicinal* protons unaffected. The comparison between these two types of relaxation experiments is expected to reveal the effects of *vicinal* protons on the determination of the spectral densities.

In the present investigation the following five different Grant-type initial perturbations for the $^{13}\text{CH}_2\text{M}$ spin system were used: (1) a ^{13}C 180° pulse inverting the entire methylene triplet (abbreviated to CP), (2) a ^1H 180° pulse inverting the proton doublet (denoted by PP for brevity), (3) selective ^1H 180° pulse inverting the only the upfield line of the ^1H doublet (SP), (4) a *J*-negative pulse inverting the outer lines of the ^{13}C triplet (JN), and (5) a *J*-positive pulse inverting the central line of the ^{13}C triplet (JP). Besides these, we have applied the following five different BIRD-type initial perturbations for the $^{13}\text{CH}_2\text{M}$ spin system: (1) a ^{13}C 180° pulse inverting the entire methylene triplet and a ^1H 180° pulse inverting the only neighboring protons (CPB), (2) a ^1H 180° pulse inverting the only protons of $^{13}\text{CH}_2$ (PPB), (3) a ^{13}C 180° pulse inverting the entire methylene triplet and a ^1H 180° pulse inverting the only protons of $^{13}\text{CH}_2$ (CPPB), (4) a *J*-negative pulse inverting the outer lines of the ^{13}C triplet and a ^1H 180° pulse inverting the only protons of $^{13}\text{CH}_2$ (JNB), (5) a *J*-positive pulse inverting the central line of the ^{13}C triplet and a ^1H 180° pulse inverting only the protons of $^{13}\text{CH}_2$ (JPB).

Calculations and Relaxation Curve Fittings. Relaxation parameters were obtained through a multiparameter least-squares curve fitting of observed relaxation data with those derived from Eq. (4). We have used the Levenberg-Marquardt algorithm for searching the minima throughout these curve-fitting procedures.^{21,22} To account for systematic instrumental errors, differences in T_2^* relaxation of each line during the pulse sequences, and pulse imperfections we parameterized the initial values of the normal modes. For

Table 1. Best Fitted Spectral Densities for [5- ^{13}C] *n*-Undecane

	AX_2^a	AX_2^b	AX_2M^b
J_{CH}	0.0369 ± 0.0008	0.0347 ± 0.0020	0.0305 ± 0.0003
J_{HCH}	0.0043 ± 0.0036	0.0041 ± 0.0086	0.0026 ± 0.0021
J_{CHH}	0.0218 ± 0.0010	0.0210 ± 0.0026	0.0228 ± 0.0004
J_{HH}	0.0335 ± 0.0017	0.0310 ± 0.0048	0.0447 ± 0.0009
j_c	[0.0] ^c	0.0088 ± 0.0091	$[0.0114 \pm 0.0005]^d$
j_H	0.0789 ± 0.0034	0.0808 ± 0.0096	0.0615 ± 0.0016
j_{HH}	0.0500 ± 0.0186	0.0554 ± 0.0445	0.0163 ± 0.0085
Γ_{116}			0.0114 ± 0.0005
Γ_{216}			0.0354 ± 0.0033
Γ_{1616}			0.2787 ± 0.0094
χ^2/N	9.94×10^{-5}	1.03×10^{-4}	2.02×10^{-4}

^a AX_2 denotes the results of the AX_2 model fit of the relaxation data obtained by applying the Grant type pulses only. ^b AX_2M denotes the results of the AX_2M model fit of the relaxation data obtained by both the Grant and BIRD-type pulses. ^cSquare bracket denotes that the value was kept fixed during the fit. ^dSquare bracket denotes that random field term for ^{13}C was assumed to originate only from dipolar term between ^{13}C and *M* proton.

this, we first guessed a set of rough initial values for these normal modes and fitted the relaxation data using the relaxation matrix elements obtained in the case of AX_2 model, to find a more refined set of initial values. These initial values are then fed back to find a set of matrix elements that produces better curve fittings. This procedure was continued until the self-consistent best-fitted parameters were obtained. In particular the starting initial value for ${}^a\nu_M$ was set to -1 when a hard 180° proton pulse was applied but to 0 when a BIRD-type selective 180° proton pulse was applied.

Results and Discussion

To interpret the observed data we first tried to fit the relaxation data obtained by applying only the Grant-type pulse sequences with the relaxation curves derived on the basis of AX_2 model. This resulted in a good fit, yielding a set of spectral density values as shown in Table 1 (but not graphically shown). However, use of these spectral density values failed to reproduce the relaxation data obtained by applying the BIRD-type pulse sequences very well as shown also in Figure 4, which indicates that our methylene moiety is not so simple as to be satisfactorily described as a simple AX_2 system. In other words, this is to say that the effect of the *vicinal* protons on $^{13}\text{CH}_2$ relaxation cannot be approximated as arising from random field terms only.

In order to get over this hurdle we invoked the AX_2M model that was described in the previous section, which yielded successful simultaneous fittings with both types of relaxation data as shown in Figure 5. In these calculations the modes ν_9 through ν_{15} except ${}^a\nu_M$ were ignored during the relaxation as we had reasoned in the previous section. Although we treat our system on the basis of an AX_2M model, it is not a truly isolated AX_2M system, however, because all the spins involved are more or less are interacting with other surrounding protons. In particular, the

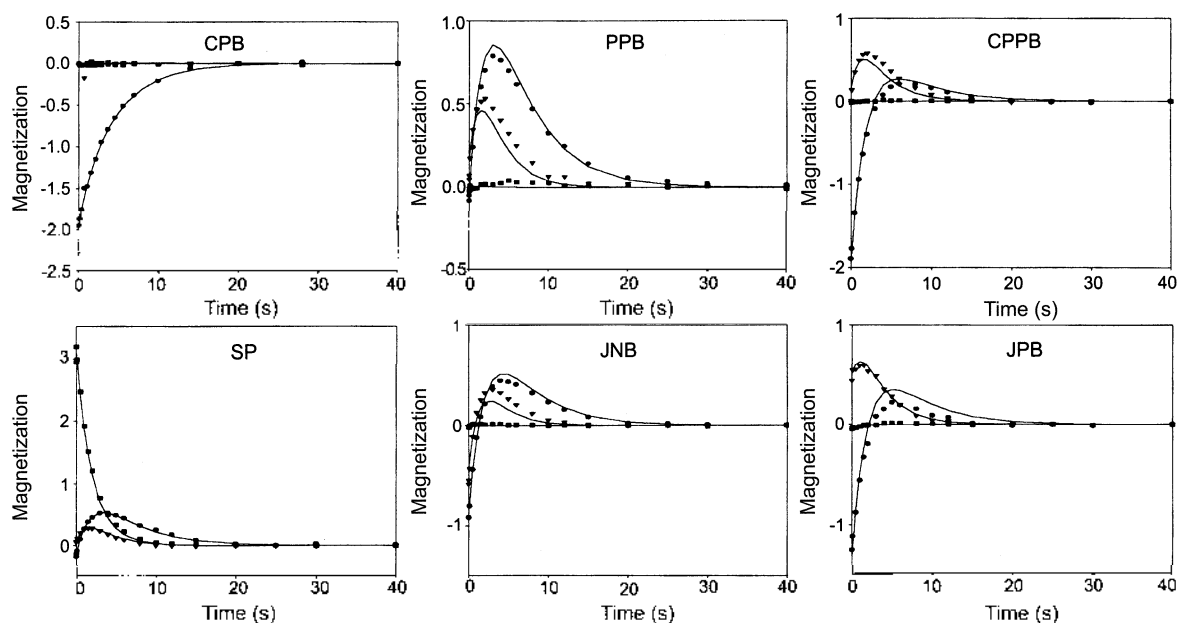


Figure 4. Plot of Magnetization Modes Obtained from the Corresponding Coupled ^{13}C Spectra. The symbols denote the experimental data obtained by applying the BIRD type pulse sequences and solid lines are the curves fitted to these on the basis of the AX_2 relaxation matrix obtained from the Grant type experiments. ● : $^a\nu_1$ mode, ▼ : $^b\nu_3$ mode, ■ : $^c\nu_5$ mode

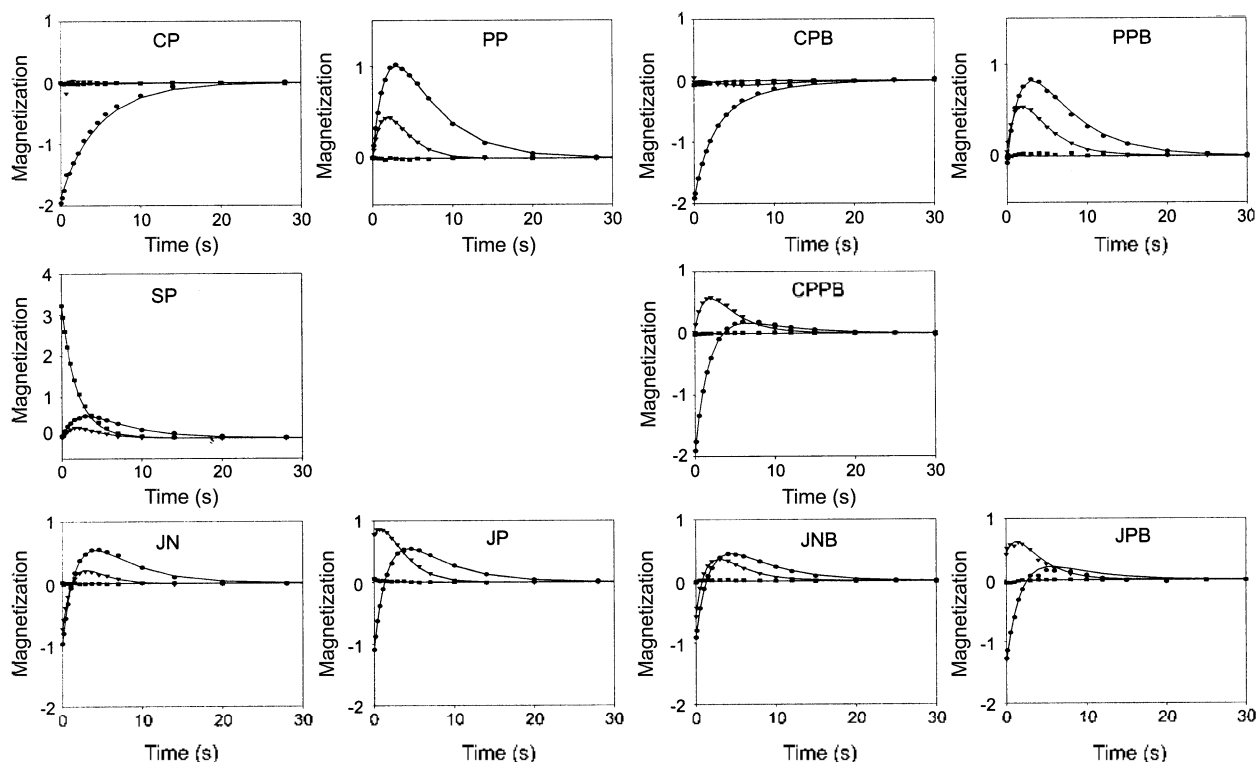


Figure 5. Plot of Magnetization Modes Obtained from Corresponding Coupled ^{13}C Spectra. The symbols denote the experimental data and solid lines represent the curves fitted to these on the basis of AX_2M relaxation model. ● : $^a\nu_1$ mode, ▼ : $^b\nu_3$ mode, ■ : $^c\nu_5$ mode

spin M has another independent efficient relaxation pathway through interactions with the surrounding protons other than AX_2 spins. To account for this we have introduced an additional element $1/T_1$ in the column of relaxation matrix that relates the $^a\nu_1$ mode with other modes. In the proton spectrum of our sample molecule n -undecane M spin

displays a somewhat broad, not well-resolved peak and this peak is found to decay nearly exponentially when inverted by a hard 180° pulse, which enables us to estimate a crude value of T_1 . This value could be further refined through the curve fitting procedure as already described.

The spectral density values obtained through the least-

squares curve fitting procedure are listed in Table 1. We see from these that the various spectral density data calculated on the basis of the AX_2 model are affected substantially if the presence of *vicinal* protons is taken into consideration. The *vicinal* protons are expected to make their presence felt by the carbon of our interest *via* direct dipole-dipole interactions as well as random field interactions. Although two groups of *vicinal* protons around the carbon labeled at the [5] position in undecane may be motionally inequivalent, we found that only two parameters are needed to describe satisfactorily the effect due to *vicinal* protons in our case. That is, we had $J_{CM} = 0.00171$ (5.6% of J_{CH}) and $J_{HM} = 0.00375$ (8.4% of J_{HH}) on the average for each of four *vicinal* protons. Our success may be due to the fact that the effect arising from the *vicinal* protons is merely secondary to that of the *geminal* protons, so that the small difference in J_{CM} and J_{HM} between the two groups of *vicinal* protons does not make significant contribution to the fitting results. These parameters are small in magnitude compared with J_{CH} and J_{HH} , respectively, but large enough to indicate that the effect of *vicinal* protons cannot be fully described by random field interactions only. And all the spectral density values deduced from the fitting results differ from the case of AX_2 model by more than 5%.²³

One conventional method that is usually considered to minimize the effect due to *vicinal* protons is to deuterate them. However, this method is not easy to be applied for the type of experiments we described here, because not only the *vicinal* protons should be deuterated but at the same time the carbon of interest must be isotopically labeled as well for the sake of signal intensity. Fuson *et al.* have discussed the effect of *vicinal* protons on the relaxation of central carbon in *n*-nonane by comparing the measured data for deuterated and nondeuterated compound. They have also found that J_{CH} decreases only slightly in the presence of *vicinal* protons and have recommended that J_{CH} values calculated from the AX_2 model can be used for the study of molecular dynamics without much ado. However, the deuterated nonane molecule that they have used for comparison is a heavily deuterated species; *i.e.* the molecule in which all the protons, let alone the *vicinal* protons, except those in central methylene moiety of interest were deuterated. Such a heavily deuterated molecule may exhibit somewhat different dynamical behavior in comparison with a non-deuterated species due to increased mass and moment of inertia. Therefore, it remains to be seen that deuteration is a sure way to eliminate the uncertainty in the values of various spectral densities. In this respect the method we propose in this paper may be considered to provide a viable way of serving for this purpose.

Acknowledgment. This research was financially supported by the BK21 project of the Ministry of Education, Korea.

Appendices

I. Relaxation matrix elements for AX_2M

$$\Gamma_{11} = 20/3J_{CH} + 10/3J_{CM} + 2j_C \quad \Gamma_{12} = 5\sqrt{2}/3J_{CH}$$

$$\begin{aligned} \Gamma_{13} &= 2J_{HCH} \quad \Gamma_{14} = 7\sqrt{2}/3J_{HCH} \\ \Gamma_{113} &= 2\sqrt{2}J_{HCM} \quad \Gamma_{116} = 5/3J_{CM} \\ \Gamma_{22} &= 10/3J_{CH} + 5J_{HH} + 10/3J_{HM} + 2j_H \\ \Gamma_{23} &= 2\sqrt{2}J_{CHH} \quad \Gamma_{24} = 5/3J_{HCH} - 2J_{CHH} \quad \Gamma_{213} = 2J_{CHM} \\ \Gamma_{214} &= 2\sqrt{2}J_{HHM} \quad \Gamma_{215} = -2J_{HHM} + 5/3J_{HMH} \\ \Gamma_{216} &= 5\sqrt{2}/3J_{HM} \\ \Gamma_{33} &= 4J_{CH} + 10/3J_{CM} + 2J_{HH} + 20/3J_{HM} + 2j_C + 4j_H \\ \Gamma_{34} &= -\sqrt{2}J_{HCH} - \sqrt{2}J_{HH} - 10\sqrt{2}/3J_{HMH} - 2\sqrt{2}j_{HH} \\ \Gamma_{313} &= 2\sqrt{2}J_{HCM} + 2\sqrt{2}J_{HHM} + 5\sqrt{2}/3J_{HM} \\ \Gamma_{314} &= 4J_{CHM} + 5/3J_{CM} \quad \Gamma_{315} = -2\sqrt{2}J_{CHHM} \\ \Gamma_{44} &= 14/3J_{CH} - 4/3J_{HCH} + 10/3J_{CM} + J_{HH} + 20/3J_{HM} \\ &\quad - 10/3J_{HMH} + 2j_C + 4j_H - 2j_{HH} \\ \Gamma_{413} &= -2J_{HHM} - 5/3J_{HMH} \quad \Gamma_{414} = -2\sqrt{2}J_{CHHM} \\ \Gamma_{415} &= 14/3J_{CHM} - 8/3J_{CHHM} + 5/3J_{CM} \\ \Gamma_{55} &= 16/3J_{CH} + 2J_{HCH} + 10/3J_{CM} + 5J_{HH} + 10/3J_{HM} + 2j_C \\ &\quad + 2j_H \\ \Gamma_{56} &= 5\sqrt{2}/3J_{CH} + 2\sqrt{2}J_{CHH} \quad \Gamma_{57} = -5/3J_{HCH} - 2J_{CHH} \\ \Gamma_{59} &= 2\sqrt{2}J_{HCM} + 5\sqrt{2}/3J_{HM} \quad \Gamma_{510} = 2J_{CHM} + 5/3J_{CM} \\ \Gamma_{511} &= 2\sqrt{2}J_{HCM} + 2\sqrt{2}J_{HHM} \quad \Gamma_{512} = -2J_{HHM} + 5/3J_{HMH} \\ \Gamma_{66} &= 20/3J_{CH} + 2J_{HH} + 20/3J_{HM} + 4j_H \\ \Gamma_{67} &= -10\sqrt{2}/3J_{HCH} - \sqrt{2}J_{HH} - 10\sqrt{2}/3J_{HMH} - 2\sqrt{2}j_{HH} \\ \Gamma_{610} &= 2\sqrt{2}J_{HHM} + 5\sqrt{2}/3J_{HM} \quad \Gamma_{611} = 4J_{CHM} \\ \Gamma_{612} &= -2\sqrt{2}J_{CHHM} \\ \Gamma_{77} &= 20/3J_{CH} - 10/3J_{HCH} + J_{HH} + 20/3J_{HM} - 10/3J_{HMH} + 4j_H \\ &\quad - 2j_{HH} \\ \Gamma_{710} &= -2J_{HHM} - 5/3J_{HMH} \quad \Gamma_{711} = -2\sqrt{2}J_{CHHM} \\ \Gamma_{712} &= 14/3J_{CHM} - 8/3J_{CHHM} \\ \Gamma_{99} &= 20/3J_{CH} + 2J_{CM} + 20/3J_{HM} + 2j_C + 2j_M \\ \Gamma_{910} &= 5\sqrt{2}/3J_{CH} + 2\sqrt{2}J_{CMH} \quad \Gamma_{911} = 2J_{HCH} + 2J_{HMH} \\ \Gamma_{912} &= 7\sqrt{2}/3J_{HCH} + 7\sqrt{2}/3J_{HMH} \\ \Gamma_{1010} &= 10/3J_{CH} + 10/3J_{CM} + 5J_{HH} + 16/3J_{HM} + 2J_{HMH} + 2j_H \\ &\quad + 2j_M \\ \Gamma_{1011} &= 2\sqrt{2}J_{CHH} + 2\sqrt{2}J_{CMH} \quad \Gamma_{1012} = 5/3J_{HCH} - 2J_{CHH} \\ \Gamma_{1111} &= 4J_{CH} + 2J_{CM} + 2J_{HH} + 4J_{HM} + 2j_C + 4j_H + 2j_M \\ \Gamma_{1112} &= -\sqrt{2}J_{HCH} - \sqrt{2}J_{HH} - \sqrt{2}J_{HMH} - 2\sqrt{2}j_{HH} \\ \Gamma_{1212} &= 14/3J_{CH} - 4/3J_{HCH} + 2J_{CM} + J_{HH} + 14/3J_{HM} - 4/3J_{HMH} \\ &\quad + 2j_C + 4j_H - 2j_{HH} + 2j_M \\ \Gamma_{1313} &= 16/3J_{CH} + 2J_{HCH} + 2J_{CM} + 5J_{HH} + 16/3J_{HM} + 2J_{HMH} \\ &\quad + 2j_C + 2j_H + 2j_M \\ \Gamma_{1314} &= 5\sqrt{2}/3J_{CH} + 2\sqrt{2}J_{CHH} + 2\sqrt{2}J_{CMH} \\ \Gamma_{1315} &= -5/3J_{HCH} - 2J_{CHH} \\ \Gamma_{1316} &= 2\sqrt{2}J_{CMH} \end{aligned}$$

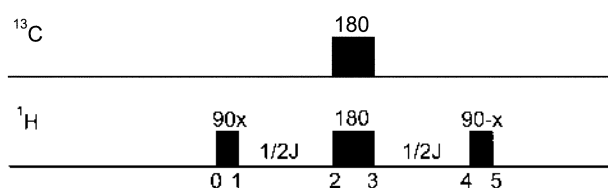


Figure A1. A BIRD Pulse Sequence.

$$\Gamma_{1414} = 20/3 J_{CH} + 10/3 J_{CM} + 2J_{HH} + 4J_{HM} + 4j_H + 2j_M$$

$$\Gamma_{1415} = -10\sqrt{2}/3 J_{HCH} - \sqrt{2} J_{HH} - \sqrt{2} J_{HMH} - 2\sqrt{2} j_{HM}$$

$$\Gamma_{1416} = 2J_{HMH}$$

$$\Gamma_{1515} = 20/3 J_{CH} - 10/3 J_{HCH} + 10/3 J_{CM} + J_{HH} + 14/3 J_{HM}$$

$$- 4/3 J_{HMH} + 4j_H - 2j_{HH} + 2j_M \quad \Gamma_{1516} = 7\sqrt{2}/3 J_{HMH}$$

$$\Gamma_{1616} = 10/3 J_{CM} + 20/3 J_{HM} + 2j_M$$

II. Action of BIRD Pulse on AX₂Y Spin System

We analyze here the action of the BIRD-type pulses shown in Figure A1 on an AX₂Y spin system in which the spin coupling between A and X spins is much larger than both the spin coupling and the chemical shift difference between X and Y protons as well as the spin coupling between A and Y spin.

At equilibrium and after the first 90° proton pulse, the density operators are, respectively, written as

$$\sigma_0 = \alpha I_z - S_{1z} + S_{2z} + T_z, \quad (A1)$$

$$\sigma_1 = \alpha I_z - S_{1y} - S_{2y} - T_y, \quad (A2)$$

where *I*, *S* and *T* are the angular momentum operators for carbon-13, *geminal* protons and a *vicinal* proton and α is γ/γ_1 with γ standing for the magnetogyric ratio of a nucleus of the given kind. After a BIRD pulse sequence, the density operator becomes

$$\sigma_5 = P(\pi/2)_x L C(\pi) P(\pi)_x L \sigma_1 L^* P(\pi)_x^* C(\pi)^* L^- P(\pi/2)_x^-, \quad (A3)$$

where $P(\pi/2)_x$, $P(\pi)_x$, and $C(\pi)$ are, respectively, the operators describing the action of hard proton and carbon pulses; that is,

$$P(\pi/2)_x = \exp[-i(\pi/2)(S_{1x} + S_{2x} + T_x)],$$

$$P(\pi)_x = \exp[-i\pi(S_{1x} - S_{2x} + T_x)], \text{ and}$$

$$C(\pi)_x = \exp(-i\pi I_x). \quad (A4)$$

L is the operator for free evolution between two successive pulses; that is,

$$L = \exp(-iH\tau) \quad (A5)$$

where *H* is the spin Hamiltonian for the given spin system and τ is the evolution period between hard proton 90° and 180° pulse. The spin Hamiltonian for the system may be written in the form

$$H = H_\omega + H_J, \quad (A6)$$

where H_ω and H_J are, respectively, the chemical shift part

and the spin coupling part of the Hamiltonian expressed in unit of \hbar ; that is,

$$H_\omega = \omega_x I_x + \omega_Y(S_{1z} + S_{2z}) + \omega_Y T_z, \quad (A7)$$

and

$$H_J = \pi J \cdot 2I_z(S_{1z} + S_{2z}) - \pi J' \cdot 2I_z T_z + \pi J'' \cdot 2(S_1 - S_2) \cdot T \quad (A8)$$

with the following definitions:

ω_x = chemical shift frequency of carbon,

ω_Y = chemical shift frequency of *geminal* protons,

ω_Y = chemical shift frequency of *vicinal* proton,

J = spin coupling constant between carbon and *geminal* protons,

J' = spin coupling constant between carbon and *vicinal* proton,

and

J'' = spin coupling constant between *geminal* and *vicinal* protons.

On action of simultaneous hard proton and carbon 180° pulses the coupling part H_J remains invariant while the chemical shift part changes its sign, and, therefore, we may rewrite (A3) as

$$\sigma_5 = P(\pi/2)_x L L' C(\pi) P(3\pi/2)_x \sigma_1 P(3\pi/2)_x^* C(\pi)^* (LL')^- P(\pi/2)_x^-, \quad (A9)$$

where

$$LL' = \exp[-i(H_\omega + H_J)\tau] \exp[-i(-H_\omega + H_J)\tau] \quad (A10)$$

Since H_ω does not commute with H_J , two exponent operators in (A10) do not commute either and it is troublesome to deal with the operator LL' . However, we can deal with this operator approximately using the following formula:²¹

$$\exp(-iM\tau) \exp(-iN\tau) = \exp\left[-i(M+N)\tau - \frac{\tau^2}{2}[M, N] - i\frac{\tau^3}{6}[M, [M, N]] + \dots\right], \quad (A11)$$

where $M = -H_\omega + H_J$ and $N = H_\omega - H_J$.

For $\tau = 1/2J$ the magnitude of the second term in the exponent series in (A11) can be shown to be of the order of $(\Delta\omega J''/J)^2$ where $\Delta\omega$ is the chemical shift difference between *vicinal* and *geminal* protons. For our system *J* is much larger than both $\Delta\omega$ and J'' and therefore the second and ensuing terms may safely be ignored. This amounts to writing

$$LL' = \exp(-2iH_J\tau) \quad (A12)$$

H_J operator itself still consists of two non-commuting parts, but by the same logic as we have used for deriving (A12) we can show that

$$LL' \approx \exp[-4\pi J I_z(S_{1z} + S_{2z})\tau] \exp(-4\pi i J' I_z T_z \tau) \exp[-4\pi i J''(S_1 + S_2) \cdot T \tau] \quad (A13)$$

On substituting (A13) into (A9), we see that for $\tau = 1/2J$ the carbon signal associated with proton zero-quantum coherence involving *geminal* and *vicinal* protons can arise if the non-

secular part of the spin coupling between these two protons cannot be ignored and its intensity is roughly proportional to $\sin(2\pi J'/J)\sin(2\pi J''/J)$ which is very small if J is very large compared with both J' and J'' .

References

1. Courtieu, J.; Gonord, P.; Mayne, C. L. *J. Chem. Phys.* **1980**, *72*, 953.
 2. Fuson, M. M.; Prestegard, J. H. *J. Am. Chem. Soc.* **1983**, *105*, 168.
 3. Fuson, M. M.; Prestegard, J. H. *Biochemistry* **1983**, *22*, 1311.
 4. Brown, M. S.; Grant, D. M.; Horton, W. J.; Mayne, C. L.; Evans, G. T. *J. Am. Chem. Soc.* **1985**, *107*, 6698.
 5. Fuson, M. M.; Grant, D. M. *Macromolecules* **1988**, *21*, 944.
 6. Fuson, M. M.; Grant, D. M. *Macromolecules* **1991**, *24*, 2594.
 7. Grant, D. M.; Mayne, C. L.; Liu, F.; Xiang, T.-X. *Chem. Rev.* **1991**, *91*, 1591.
 8. Zheng, Z.; Mayne, C. L.; Grant, D. M. *J. Magn. Reson. A* **1993**, *103*, 268.
 9. Xiang, T.-X.; Liu, F.; Grant, D. M. *J. Chem. Phys.* **1991**, *95*, 7576.
 10. Liu, F.; Horton, W. J.; Mayne, C. L.; Xiang, T.-X.; Grant, D. M. *J. Am. Chem. Soc.* **1992**, *114*, 5281.
 11. Fuson, M. M.; Belu, A. M. *J. Magn. Reson.* **1994**, *107*, 1.
 12. Liu, F.; Mayne, C. L.; Grant, D. M. *J. Magn. Reson.* **1989**, *84*, 344.
 13. Vax, A. *J. Magn. Reson.* **1983**, *53*, 517.
 14. Redfield, A. G. *IBA J. Res. Develop.* **1957**, *1*, 19.
 15. Redfield, A. G. *Adv. Magn. Reson.* **1965**, *1*, 1.
 16. Solomon, I. *Phys. Rev.* **1955**, *99*, 559.
 17. Wang, C. H.; Grant, D. M. *J. Chem. Phys.* **1976**, *64*, 1522.
 18. Pyper, N. C. *Mol. Phys.* **1971**, *21*, 1.
 19. Pyper, N. C. *Mol. Phys.* **1971**, *22*, 433.
 20. Werbelow, L. G.; Grant, D. M. *Adv. Magn. Reson.* **1977**, *9*, 189.
 21. Bevington, P. R. *Data Reduction and Error Analysis for the Physical Sciences*; McGraw-Hill: 1969.
 22. Press, W. H.; Flannery, B. P.; Teukolsky, S. A.; Vetterling, W. T. *Numerical Recipes-The Art of Scientific Computing*; Cambridge University Press: 1986.
 23. Namgoong, H.; Lee, I.; Lee, J. W. *Bull. Korean Chem. Soc.* **2000**, *21*, 1077.
 24. Goldberger, M. L.; Adams II, E. N. *J. Chem. Phys.* **1952**, *20*, 240.
-